Wang et al. Nanoscale Research Letters (2017) 12:66
DOI 10.1186/s11671-017-1826-1

Nanoscale Research Letters

NANO EXPRESS Open Access

Effect of Paclitaxel-Mesoporous Silica Nanoparticles with a Core-Shell Structure on the Human Lung Cancer Cell Line A549

Tieliang Wang[1], Ying Liu[2] and Chao Wu[2*]

Abstract

A nanodrug delivery system of paclitaxel-mesoporous silica nanoparticles with a core-shell structure (PAC-csMSN) was used to increase the dissolution of paclitaxel (PAC) and improve its treatment of lung cancer. PAC was loaded into the core-shell mesoporous silica nanoparticles (csMSN) by the adsorption equilibrium method and was in an amorphous state in terms of its mesoporous structure. In vitro and in vivo studies showed that csMSN increased the dissolution rate of PAC and improved its lung absorption. The area under concentration-time curve (AUC) value of PAC-csMSN used for pulmonary delivery in rabbits was 2.678-fold higher than that obtained with the PAC. After continuous administration for 3 days, a lung biopsy showed no signs of inflammation. Cell apoptosis results obtained by flow cytometry indicated that PAC-csMSN was more potent than pure PAC in promoting cell apoptosis. An absorption investigation of PAC-csMSN in A549 cells was carried out by transmission electron microscopy (TEM) and laser scanning confocal microscopy (LSCM). The obtained results indicated that the cellular uptake was time-dependent and csMSN was uptaken into the cytoplasm. All these results demonstrate that csMSN have the potential to achieve pulmonary inhalation administration of poorly water-soluble drugs for the treatment of lung cancer.

Keywords: Mesoporous silica nanoparticles, Paclitaxel, A549 cells, Dissolution, Pulmonary delivery

Background

Most anticancer drugs are water-insoluble, and the poor solubility seriously restricts their absorption. Classical treatment for lung cancer involves oral or intravenous administration of antifungal drug formulations [1–3]. However, these compounds have many side effects and are not very effective [4]. For these common routes of administration, a stable and efficient lung drug concentration is not always guaranteed due to low solubility and/or poor tissue penetration, which may also lead to a poor survival prognosis. Pulmonary delivery is an interesting choice because it delivers anticancer drugs directly to the cancerous tissue while maintaining high lung drug concentrations and reducing systemic side effects [5, 6].

PAC, an effective anticancer drug, is poorly water-soluble (solubility in water is 6 ng/ml). Therefore, how to improve the solubility of PAC has become an important challenge. Currently, some methods are available for improving PAC solubility, such as the use of micelles, liposomes, and nanoparticles [7–9]. With the development of nanotechnology, the application of mesoporous materials for improving the solubility of poorly water-soluble drugs is attracting wide attention. Zongzhe zhao et al. have reported the development of mesoporous silica materials in improving the solubility of fenofibrate and regulating its release rate [10]. Peng zhao et al. apply mesoporous carbon materials to increase the dissolution rate of poorly water-soluble drugs [11]. Porous hydroxyapatite, porous alumina, and porous titanium dioxide materials have also been used to improve the water solubility of insoluble drugs [12–14].

In our research, we have developed a csMSN-based PAC nanodrug delivery system for improving the treatment of lung cancer. There are two reasons for choosing csMSN as carrier for improving PAC solubility. Firstly, the spatial confinement effect of the mesoporous structure can reduce the drug particle size and increase the

* Correspondence: wuchao27@126.com
[2]Pharmacy School, Jinzhou Medical University, 40 Songpo Road, Linghe District, Jinzhou, Liaoning Province 121000, China
Full list of author information is available at the end of the article

specific surface area of the drug particles. According to the Noyes-Whitney and Ostwald-Freundlich equations, this would increase the dissolution rate of PAC. Secondly, csMSN has a regular shape, low density, and good flowability which make them suitable as a carrier for pulmonary delivery. In the work, we wished to investigate whether csMSN could be used as a pulmonary delivery carrier using a lung absorption study at a cellular level.

Methods

Materials

PAC was provided by the Dalian Meilun Company with a purity >99%. Acetonitrile, anhydrous ethanol, butylparaben, Tween 80, tetraethylorthosilicate (TEOS), aminopropyltriethoxysilane (APTES), glutaraldehyde, hypromellose, hexadecyl trimethyl ammonium bromide (CTAB), ammonia, methyl tert-butyl ether, and dichloromethane were obtained from the Jin Zhou Xing Bei reagent company. Fluorescein isothiocyanate (FITC), Hoechst 33342, rhodamine phalloidin and 3-(4,5-Dimethylthiazol-2-yl)-2,5-diphenyltetrazolium (MTT) were purchased from Beijing Dingguo Changsheng Biotechnology Co., Ltd. Deionized water was used in all experiments.

Synthesis of csMSN

csMSN was prepared according to the process reported by Wu et al. [15]. Firstly, ethanol, deionized water, and ammonia (180:65:4.5, *v*/*v*/*v*) were mixed in a glass container under stirring. Then, TEOS (15 ml) was slowly dripped into the solution. The reaction was carried out for 4 h and then solid silica nanoparticles (SSN) were obtained by centrifugation at 9500 rpm for 20 min. The product was then dried at 40 °C. Secondly, ethanol, deionized water, CTAB, and the dried SSN (13:30:150:100, *v*/*v*/*m*/*m*) were mixed in a glass container and stirred for 30 min under ultrasonication. Ammonia (0.45 ml) and TEOS (0.3 ml) were then added to the system and stirred at room temperature for 6 h. The precipitate obtained by centrifugation was washed repeatedly with ethanol and water, and then dried at 40 °C. csMSN was obtained by calcination at 550 °C.

Drug-loading Procedure

PAC, an anticancer drug, is used clinically to treat ovarian cancer, breast cancer, lung cancer, and colorectal cancer. It was chosen as a model drug and was loaded onto csMSN by the adsorption equilibrium method [16]. The drug loading of csMSN was concentration-dependent. The same amount of csMSN was soaked in different concentrations of PAC dichloromethane solution and then the suspension was stirred for 5 h. The supernatant was removed by centrifugation at 10,000 rpm and, finally, the drug-loaded sample (PAC-csMSN) was dried in a vacuum. The drug content was determined by high-performance liquid chromatography (HPLC) (L-2400, HITACHI, Japan). The drug loading (DD) of csMSN was calculated by the formula:

$$DD = \text{the amount of drug in PAC–csMSN} / \text{the amount of PAC–csMSN.}$$

Characterization of csMSN and PAC-csMSN

The structure and morphology of csMSN was observed by transmission electron microscopy (TEM; Tecnai G2F30) and scanning electron microscopy (SEM; JEOL JSM-7001F). The adsorption analyzer (SA3100, Beckman Coulter Inc., Brea, CA, USA) was used to detect the specific surface area and pore size of csMSN. The phase transition process of PAC in all samples was performed using differential scanning calorimetry (DSC; Shimadzu DSC-60, Japan) at a heating rate of 10 °C/min from 25 to 350 °C under a nitrogen flow of 150 ml/min. X-ray diffraction analysis (XRD; Rigaku Geigerflex XRD, Co., Japan,) was used to further investigate the physical state of PAC in csMSN. The step length was 0.02° and the scanning rate was 4°/min from 3° (2θ) to 60°. FTIR spectra were recorded for analyzing the interaction PAC and csMSN using an FT-IR spectrometer (Bruker IFS 55, Switzerland) over 400 to 4000 cm^{-1} using the KBr pellet technique.

In Vitro Drug Dissolution

Dissolution testing was performed using a USP dissolution apparatus type II (RC-8D, Tianjin Guoming Medical Equipment Co., Ltd.). The dissolution medium was pH 7.4 phosphate buffer with 1% Tween 80. For this, 10 mg PAC and PAC-csMSN powder containing an equivalent of 10 mg PAC were respectively put in 1000 ml dissolution medium at a temperature of 37 ± 0.5 °C and the paddle speed was 100 rpm/min. Then, 5 ml samples of dissolution medium were withdrawn at 5, 10, 15, 20, 30, 45, and 60 min and passed through a 0.22 μm microporous membrane filter for HPLC analysis. The detection wavelength was 227 nm, and the mobile phase was acetonitrile and water with a volume ratio of 50:50 [17].

In Vivo Pharmacokinetic Study

Animals and Dosing

The animal experiment was approved by the Jinzhou Medical University Laboratory Animal Ethics Committee. Twelve rabbits (2.5 ± 0.5 kg) were randomly assigned to two groups for evaluating the pharmacokinetics of PAC-csMSN powder and PAC powder after pulmonary administration. After fasting for 12 h, one group was given a suspension of PAC-csMSN powder containing 2%

hypromellose (equivalent to 10 mg PAC) while the other group was given an aqueous suspension of PAC powder (10 mg) containing 2% hypromellose by the trachea cannula-instillation method [18, 19]. All rabbits had free access to drinking water throughout the study. Blood samples (3.0 ml) were collected from the ear vein at 0.5, 1, 1.5, 2, 2.5, 3, 4, 5, 6, 8, 12, and 24 h and centrifuged at 5000 rpm for 10 min. The obtained plasma samples were stored at −20 °C.

Six rabbits (2.5 ± 0.5 kg) were randomly assigned to two groups for evaluating the inhalation safety of PAC-csMSN powder and csMSN powder after pulmonary administration. The csMSN group and PAC-csMSN group received continuous administrations for 3 days, and then the lung tissues were removed for pathological study. Lung specimens were fixed with formalin and embedded into paraffin then sectioned in a thin-slice cutting machine. The obtained tissue sections were stained with hematoxylin and eosin (H&E) and observed under a fluorescent microscope.

Determination of PAC in Plasma

PAC plasma concentrations were determined by HPLC (L-2400, HITACHI, Japan) with a UV–vis detector. A Welch C18 column (4.6 mm × 200 mm, 5 μm) was used for analysis, and the mobile phase was a mixture of acetonitrile and water (50:50, *v*/*v*). Detection was carried out at a flow rate of 1 ml/min. Butylparaben was selected as the internal standard, and UV detection was performed at 227 nm [17]. Plasma samples (1 ml) were transferred to 10-ml centrifuge tubes, and then 20 μl internal standard solution (50 μg/ml) was added. After vortex mixing for 5 min, 5 ml methyl tert-butyl ether was added followed by vortexing for a further 10 min. After centrifuging at 10,000 rpm for 5 min, the organic layer of each sample was transferred to another centrifuge tube, then evaporated at 40 °C using a centrifugal drying machine (LNG-T-820, Hualida, China). The residue was dissolved in 50 μl mobile phase and centrifuged at 10,000 rpm for 5 min. Finally, 20 μl supernatant was subjected to HPLC analysis. All the pharmacokinetic data of PAC were analyzed using DAS 2.0 software.

In Vitro Cytotoxicity Assay

The MTT assay examines the mitochondrial activity of the cells which is reflected by blue formazan crystals. A549 cells were seeded in 96-well plates at a density of 1×10^5 cells per well. The cytotoxicity of csMSN, PAC, and PAC-csMSN was measured in cell monolayers by exposure to csMSN, PAC, and PAC-csMSN suspension at different concentrations for 72 h. The concentrations of csMSN were 12.5, 25, 50, 125, 250, and 500 μg/ml. According to the conversion of drug loading, the series concentration of PAC-csMSN were equivalent to 10, 20, 40, 80, 160, and 320 μg/ml of PAC concentration. MTT solution (20 μl/well) was added and incubated for 4 h. Next, DMSO (200 μl) was added and the cytotoxicity was determined by a Plate Reader (DNM-9606) at 492 nm (Tecan, Germany) [20].

The Flow Cytometry Assays

A549 cells were seeded in 6-well plates, and a density was 1×10^5 cells per well. After cells had attached and proliferated for 24 h, the culture medium was removed and the adherent cells were washed with PBS. A549 cells treated with serum-free 1640 culture medium were used as a control. PAC (5, 10 ng/ml) and PAC-csMSN (equivalent to 5 and 10 ng/ml of PAC concentration) were added and incubated for 24 h. Treated A549 cells were washed three times with PBS, then harvested by trypsinization. The cells collected by centrifugation were suspended in 500 μl binding buffer. Next, 5 μl Annexin V-FITC and 5 μl PI (Nanjing Jiancheng Biological Science and Technology Co., Ltd., China) were added and incubated for 15 min at room temperature in the dark [8]. The apoptosis of A549 cells was determined by flow cytometry (Becton Dickinson, CA).

Preparation of FITC-csMSN and LSCM Observation in Uptake Experiments

The surface of csMSN with an amino group (csAMSN) was achieved by an amination reaction [21]. csMSN (500 mg) was heated in an oven at 100 °C for 30 min in order to remove water. Then, anhydrous alcohol (50 ml) was added in a three-necked flask, and APTES (2 ml) was dripped slowly into the suspension under stirring. The reaction was carried out at 77 °C for 10 h in a water bath, and the whole process was under a nitrogen atmosphere. The csAMSN was obtained by centrifugation and washed three times with ethanol and dried at 50 °C. Next, csAMSN (100 mg) was added to 1 ml FITC alcohol solution (1 mg/ml) and allowed to stand for 4 h under stirring. FITC-labeled csAMSN (FITC-csMSN) was obtained by centrifugation and dried in a vacuum.

A549 cells were seeded in 6-well plates, and a density was 5×10^4 cells per well. After cells had attached and proliferated for 48 h, the culture medium was removed and the adherent cells were washed with PBS. FITC-csMSN (50 μg/ml) was added and incubated for 0.5, 1, and 2 h. After washing three times with PBS, the A549 cells were fixed in 4% formaldehyde PBS solution for 10 min. After removing the medium and washing three times with PBS, the A549 cells were then incubated in 0.1% of Triton X-100 PBS solution containing 10% bovine serum albumin for 30 min. Then, the cells were stained with 1 μg/ml Hoechst 33342 PBS solution for 20 min, followed by Rhodamine-phalloidin PBS solution for 20 min and then washed twice with PBS [22]. Finally,

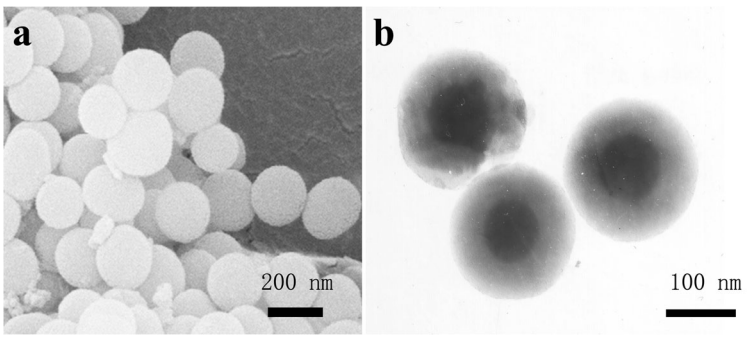

Fig 1 The SEM image of the csMSN (**a**) and the TEM image of the csMSN (**b**)

the cell uptake of FITC-csMSN was examined by laser scanning confocal microscopy (LSCM; Leica, Germany).

Transmission Electron Microscopy (TEM) Study

A549 cells were seeded in 6-well plates and a density of 5×10^4 cells per well. After the cells had attached and proliferated for 24 h, the culture medium was removed and the adherent cells were washed with PBS. csMSN (50 μg/ml) dispersed in serum-free 1640 culture medium was added to the 6-well plates and incubated for 4 h. After removing the medium, the cells were washed three times with PBS in order to detach the free csMSN. The collected cells from the 6-well plates were fixed 2% glutaraldehyde solution for 12 h at 4 °C and then embedded in 2% agarose gel. Next, A549 cells were fixed in 4% of osmium tetroxide solution. After dehydration, the cells were embedded in epoxy resin, and the embedding resin block was polymerized at 60 °C for 24 h [23]. Finally, ultrathin sections (50–70 nm) were obtained using an ultramicrotome (EMUC6, Leica, Germany) and examined by TEM.

Results and Discussion

Morphology and Structure

The morphology and structure of csMSN were examined by SEM and TEM. As seen in Fig. 1a, the SEM images clearly had a spherical appearance with an average particle size of 200 nm. The TEM image in Fig. 1b showed that csMSN had a core-shell structure. The core was solid and the shell had a mesoporous structure which made it suitable as a carrier for absorbing poorly water-soluble drugs. Its characteristics were consistent with those in the literature [15]. The specific surface area, pore size, and volume of csMSN were 585 m^2/g, 0.33 ml/g, and 5.79 nm, respectively. The space-limiting effect of the nanometer pores could restrict the size of drug particles and prevented their agglomeration. All of these factors were responsible for improving the drug dissolution. The drug loading of csMSN increased along with the PAC concentration. When the PAC concentration was more than 300 mg/ml, csMSN had the maximum drug loading (45.7 ± 1.31%).

Solid State Characterization

XRD results revealed that the PAC adsorbed into the mesoporous structure of the shell was in an amorphous form. As seen in Fig 2a, PAC-csMSN did not exhibit any characteristic crystalline reflection of PAC at 12.6° in comparison with PAC powder and the corresponding physical mixtures. The DSC results were also fully confirmed by the XRD conclusions. As shown in Fig 2b, the phase inversion temperature of PAC powder was at

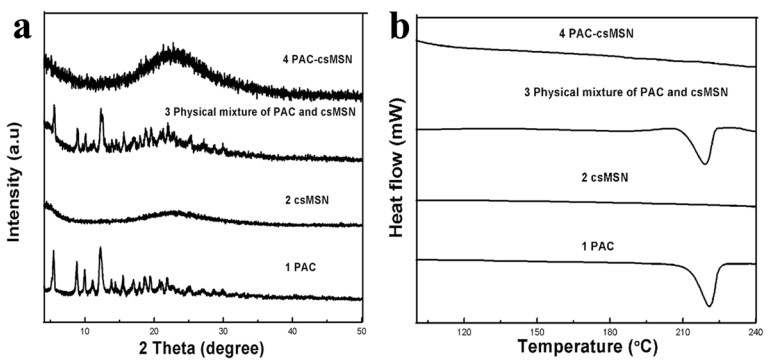

Fig 2 PAC state characterization (**a** XRD patterns, **b** DSC patterns)

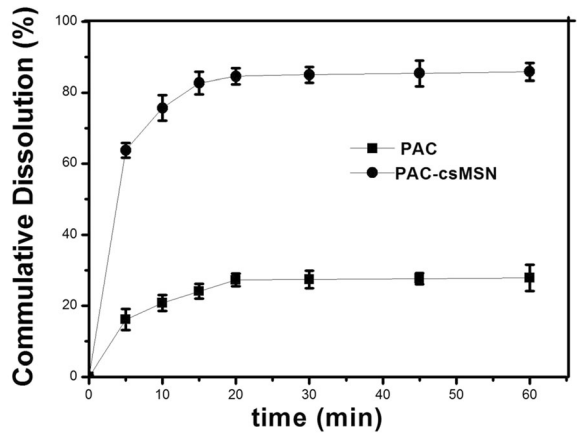

Fig 3 In vitro drug cumulative dissolution percentage patterns of PAC-csMSN powder and PAC powder ($n = 3$)

223 °C. However, the absence of a PAC melting peak in PAC-csMSN further confirmed that the PAC absorbed into csMSN existed in an amorphous state compared with that of the corresponding physical mixtures [24].

In Vitro Drug Dissolution

The effect of the mesoporous structure of csMSN on the PAC dissolution was shown in Fig. 3. The cumulative dissolution of PAC at 1 h was 27.83 ± 3.724% for PAC powder while the corresponding amount was 85.68 ± 2.585% for PAC-csMSN. Clearly, the dissolution rate was significantly improved due to the high dispersion of the shell mesoporous structure of csMSN. The reason was that PAC was present in an amorphous form because of the spatial confinement effect of the mesoporous structure [25].

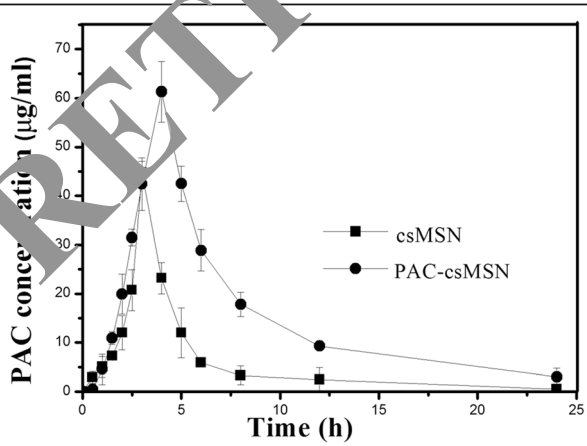

Fig 4 Plasma concentration versus time profiles after pulmonary administration of PAC-csMSN powder and PAC powder in rabbits ($n = 6$)

In Vivo Experiment

PAC concentrations were determined in rabbit plasma at different times. The concentration–time profiles were shown in Fig. 4, and the pharmacokinetic parameters were listed in Table 1. The Cmax, Tmax, and AUC of PAC-csMSN powder were 61.32 ± 13.82, 4.316 ± 1.214, and 358.4 ± 32.56 compared with 44.76 ± 8.061, 3.632 ± 0.875, and 133.8 ± 21.45 for PAC powder, which indicated that PAC-csMSN powder had a faster and greater absorption by the alveoli. This result is directly related to the amorphous nature of PAC in PAC-csMSN powder. The amorphous PAC, as demonstrated during the in vitro release test, provided a higher concentration of dissolved PAC in the surrounding lung fluid compared with the crystalline PAC powder and was immediately absorbed due to its good cell membrane permeability. Based on the Noyes–Whitney equation, the higher absorption of amorphous PAC (a BSC II class drug) was closely correlated with faster in vivo dissolution.

Pathology Study

The pathology study was used to analyze any changes in lung tissue after administration. As seen in Fig. 5a, the cells in the tissue section of the normal lung specimen of the csMSN group were uniformly spongy and the lung tissue showed no signs of edema and congestion. No macrophages were found in the alveoli. By contrast, the PAC-csMSN group in Fig. 5b also showed no inflammation, which indicated that the PAC-csMSN nanodrug delivery system was biologically safe for continuous administration in the short term.

In Vitro Cytotoxicity Assay and Apoptosis Analysis

The csMSN were incubated with A549 cells for 72 h at different concentrations (from 12.5 to 500 μg/ml). As seen in Fig. 6a, the viability of the A549 cells was above 90% at a high concentration of 500 μg/ml. These results showed that csMSN is nontoxic, which is consistent with a previous literature report [26]. For the PAC and PAC-csMSN groups, the samples were incubated with A549 cells for 72 h at different concentrations (ranging from 10 to 320 μg/ml). As seen in Fig. 6b, the viability of A549 cells in the PAC-csMSN groups decreased significantly compared with the PAC groups. The cell inhibition rate was increased from 35.21% ± 2.652 at 10 ng/ml PAC to 76.43% ± 4.634 at 320 ng/ml PAC

Table 1 The pharmacokinetic parameters of PAC and PAC-csMSN

Formulation	Cmax (μg/ml)	Tmax (h)	t1/2 (h)	AUC (μg/ml*h)
PAC	44.76 ± 8.061	3.632 ± 0.875	4.271 ± 1.174	133.8 ± 21.45
PAC-csMSN	61.32 ± 13.82	4.316 ± 1.214	5.456 ± 2.057	358.4 ± 32.56

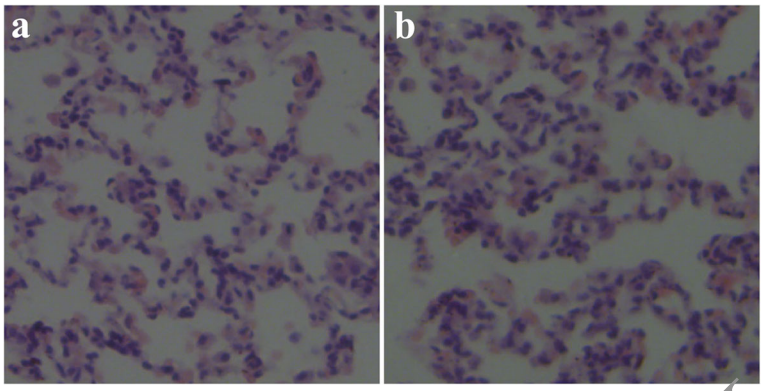

Fig 5 Lung sections after pulmonary administration of csMSN powder (**a**) and PAC-csMSN powder (**b**) in rabbits

for PAC-csMSN. These results showed that PAC-csMSN had distinct anti-proliferative effects which were concentration-dependent. The in vitro antitumor effects of PAC-csMSN can be quantitatively evaluated by IC50, which is defined as the drug concentration at which 50% of the cells have been killed in a designated time period. The IC_{50} values of PAC-csMSN groups and PAC groups were 30.74 ± 5.175 and 125.9 ± 3.762 ng/ml, respectively. These results indicated that the IC_{50} values of the PAC-csMSN groups were markedly lower ($p < 0.05$) than those of the PAC groups and the IC_{50} values of the PAC groups were four times than that of PAC-csMSN groups. The reason for this is that the mesoporous structure of csMSN can improve the solubility of PAC which allows the cells to be exposed to high concentrations of drug which inhibit cell proliferation.

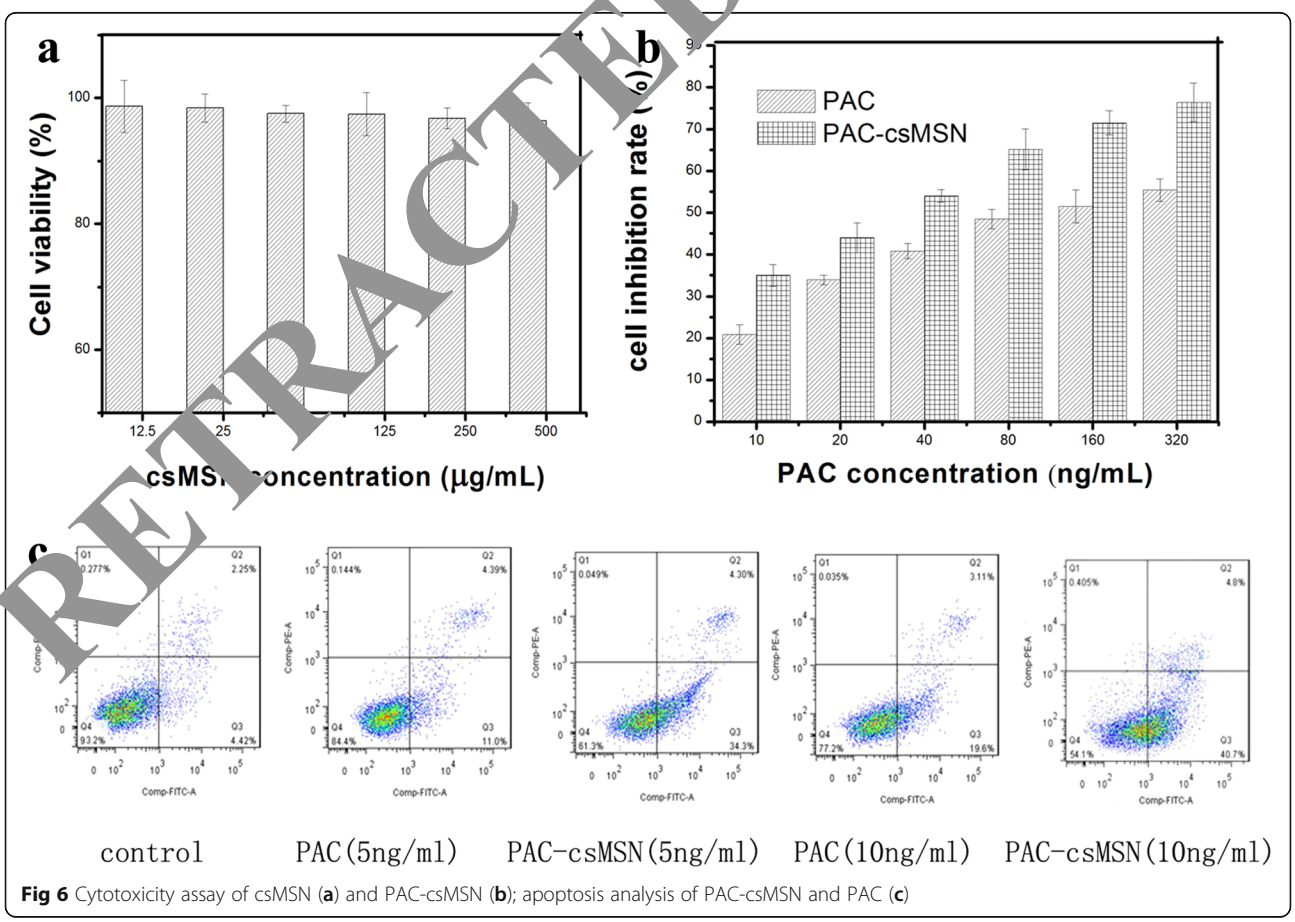

Fig 6 Cytotoxicity assay of csMSN (**a**) and PAC-csMSN (**b**); apoptosis analysis of PAC-csMSN and PAC (**c**)

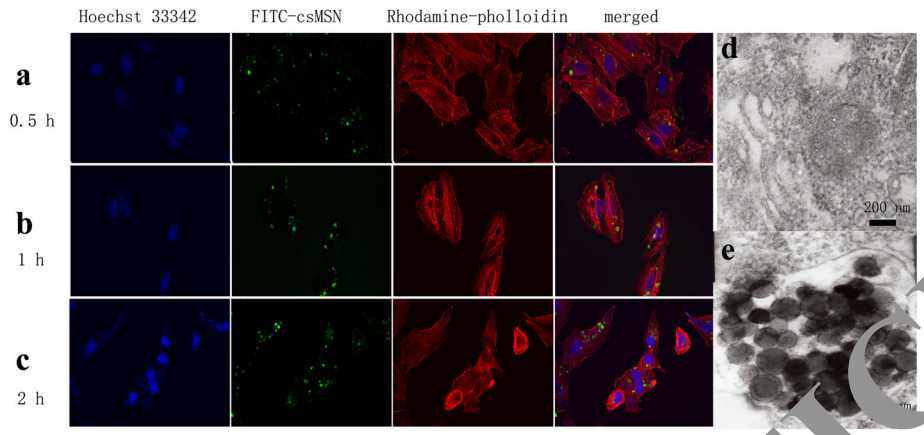

Fig 7 Cell uptake study (**a**–**c** LSCM images of FITC-csMSN, **d**, **e** TEM images of control group and csMSN group)

The analysis of apoptosis further confirmed the cytotoxicity results. As seen in Fig 6c, PAC-csMSN (34.3%) clearly promoted apoptosis compared with pure PAC (11.0%) at the same concentration (5 ng/ml) and the effect was constantly enhanced by an increase in PAC concentration. The early apoptosis rate of PAC-csMSN and pure PAC (10 ng/ml) were 19.6 and 40.7%, respectively. These results suggested that PAC-csMSN plays an important good role in promoting apoptosis.

Cell Uptake Study

The transport of FITC-csMSN was examined by LSCM. A549 cells were incubated with 50 μg/ml FITC-csMSN in serum-free 1640 medium for different times. The results obtained indicated that the cellular uptake was time-dependent. As shown in Fig 7a–c, FITC-csMSN with 200 nm were taken up into A549 cells after 0.5 h incubation at 37 °C and formed green fluorescent aggregates in the cytoplasm after 2 h. However, as time continued, FITC-csMSN did not penetrate into the nucleus despite the amount of uptake gradually increasing. The intracellular distribution of csMSN in the A549 cells was also further examined by TEM, which further supported the observed LSCM images. The possible mechanisms for the cellular uptake of csMSN involve nonspecific diffusion, phagocytosis, and endocytosis [27, 28]. As shown in Fig 7d, e, csMSN was taken up into A549 cells by endocytosis and accumulated in the vesicular or cytosolic compartment inside the A549 cells. The TEM images of ultrathin sections provide visual evidence on the cellular uptake of csMSN [29]. The results fully confirmed that the csMSN increased the absorption of drug with the aid of a nanoeffect and then to promote cell apoptosis.

Conclusions

csMSN increased the dissolution of PAC and improved PAC absorption in the lungs. PAC in PAC-csMSN was in an amorphous state in the mesoporous structure. PAC-csMSN could be taken up into the cytoplasm and promoted the apoptosis of A549 cells. All these findings demonstrate that csMSN, with good biocompatibility and biosafety, has the potential to be used as a carrier for pulmonary inhalation of PAC for the treatment of lung cancer.

Abbreviations

APTES: Aminopropyltriethoxysilane; AUC: The area under concentration-time curve; csMSN: The core-shell mesoporous silica nanoparticles; CTAB: Hypromellose, hexadecyl trimethyl ammonium bromide; DSC: Differential scanning calorimetry; FITC: Fluorescein isothiocyanate; LSCM: Laser scanning confocal microscopy; MTT: 3-(4,5-Dimethylthiazol-2-yl)-2,5-diphenyltetrazolium; PAC: Paclitaxel; PAC-csMSN: Paclitaxel-mesoporous silica nanoparticles with a core-shell structure; TEM: Transmission electron microscopy; TEOS: Tetraethylorthosilicate; XRD: X-ray diffraction analysis

Acknowledgements

This work was supported by the National Natural Science Foundation of China (no. 81302707), Principal Fund of Liaoning Medical University (no. AH2014020 and XZJJ20130104-07), and Dr. Start-up Foundation of Liaoning Province (no. 20141195).

I am very grateful to Dr. David Jack for providing the professional language services.

Funding

The National Natural Science Foundation of China (no. 81302707) and Principal Fund of Liaoning Medical University (no. AH2014020 and XZJJ20130104-07) supported the design of the study, analysis and interpretation of data. Dr. Start-up Foundation of Liaoning Province (no. 20141195) provided support in writing the manuscript.

Authors' Contributions

TW prepared carrier material and studied in vitro properties of the drug delivery system. YL was mainly responsible for cell biology research. CW designed the experimental plan. All authors read and approved the final manuscript.

Competing Interests

The authors declare that they have no competing interests.

Author details
[1]Animal Husbandry and Veterinary Medicine School, Jinzhou Medical University, 40 Songpo Road, Linghe District, Jinzhou, Liaoning Province 121000, China. [2]Pharmacy School, Jinzhou Medical University, 40 Songpo Road, Linghe District, Jinzhou, Liaoning Province 121000, China.

Received: 14 October 2016 Accepted: 30 December 2016
Published online: 23 January 2017

References

1. Reinmuth N, Meyer A, Hartwigsen D et al (2014) Randomized, double-blind phase II study to compare nitroglycerin plus oral vinorelbine plus cisplatin with oral vinorelbine plus cisplatin alone in patients with stage IIIB/IV non-small cell lung cancer (NSCLC). Lung Cancer 83:363–368
2. Naito T, Seto T, Takeda K et al (2014) Phase II clinical trial of S-1 plus oral leucovorin in previously treated patients with non-small-cell lung cancer. Lung Cancer 86:339–343
3. Sorensen SF, Carus A, Meldgaard P (2015) Intravenous or oral administration of vinorelbine in adjuvant chemotherapy with cisplatin and vinorelbine for resected NSCLC. Lung Cancer 88:167–173
4. Kobayashi H, Sato K, Niioka T et al (2015) Relationship among gefitinib exposure, polymorphisms of its metabolizing enzymes and transporters, and side effects in Japanese patients with non–small-cell lung cancer. Clin Lung Cancer 16:274–281
5. Wang RT, Zhi XY, Yao SY, Zhang Y (2015) LFC131 peptide-conjugated polymeric nanoparticles for the effective delivery of docetaxel in CXCR4 overexpressed lung cancer cells. Colloid Surface B 133:43–50
6. Kumar SP, Birundha K, Kaveri K, Devi KTR (2015) Antioxidant studies of chitosan nanoparticles containing naringenin and their cytotoxicity effects in lung cancer cells. Int J Biol Macromol 78:87–95
7. Yin TJ, Wang L, Yin LF, Zhou JP, Huo MR (2015) Co-delivery of hydrophobic paclitaxel and hydrophilic AURKA specific siRNA by redox-sensitive micelles for effective treatment of breast cancer. Biomaterials 61:10–25
8. Jiang L, Li L, He XD et al (2015) Overcoming drug-resistant lung cancer by paclitaxel loaded dual-functional liposomes with mitochondria targeting and pH-response. Biomaterials 52:126–139
9. Narayanan S, Mony U, Vijaykumar DK et al (2015) Sequential release of epigallocatechin gallate and paclitaxel from PLGA-casein core–shell nanoparticles sensitizes drug-resistant breast cancer cells. Nanomed Nanotech Nol 11:1399–1406
10. Zhao ZZ, Wu C, Zhao Y et al (2015) Development of an oral push–pull osmotic pump of fenofbrate-loaded mesoporous silica. Int J Nanomed 10:1691–1701
11. Zhao P, Wang LH, Sun CS et al (2012) Uniform mesoporous carbon as a carrier for poorly water soluble drug and its cytotoxicity study. Eur J Pharm Biophar 80:535–543
12. Zhang WD, Chai YM, Xu XH, Wang YL, Cao NN (2014) Rod-shaped hydroxyapatite with mesoporous structure as drug carriers for proteins. Appl Surf Sci 322:71–77
13. Kapoor S, Hegde R, Bhattacharyya A (2009) Influence of surface chemistry of mesoporous alumina with narrow pore distribution on controlled drug release. J Control Release 140:34–39
14. Wang TY, Jiang HT, Wang L et al (2015) Potential application of functional porous TiO2 nanoparticles for light-controlled drug release and targeted drug delivery. Acta Biomater 13:354–363
15. Wu C, Zhao ZZ, Yin Z et al (2014) Preparation of a push–pull osmotic pump of nifedipine solubilized by mesoporous silica nanoparticles with a core–shell structure. Int J Pharm 475:298–305
16. Zhao ZZ, Gao Y, Wu C et al (2015) Development of novel core-shell dual-mesoporous silica nanoparticles for the production of high bioavailable controlled-release fenofibrate tablets. Drug Dev Ind Pharm 42:199–208
17. Cha BY, Qu Y, Huang YX et al (2016) PEG-derivatized octacosanol as micellar carrier for paclitaxel delivery. Int J Pharm 500:345–359
18. Driscoll KE, Costa DL, Hatch G et al (2000) Intratracheal instillation as an exposure technique for the evaluation of respiratory tract toxicity: uses and limitations. Toxicol Sci 55:24–35
19. Ji P, Yu T, Liu Y et al (2016) Naringenin-loaded solid lipid nanoparticles: preparation, controlled delivery, cellular uptake, and pharmacokinetics in rats after pulmonary administration. Drug Des Dev Ther 10:911–925
20. Mehdi EM, Behrad D, Fatemeh AI et al (2016) Paclitaxel molecularly imprinted polymer-PEG-folate nanoparticles for targeting anticancer delivery: characterization and cellular cytotoxicity. Mat Sci Eng C-Mater 62:626–633
21. Zhang YZ, Wang JC, Bai XY et al (2012) Mesoporous silica nanoparticles for increasing the oral bioavailability and permeation of poorly water soluble drugs. Mol Pharmaceutics 9:505–513
22. Adny HS, Enio LJ, Marcelo VM et al (2016) Superparamagnetic iron-oxide nanoparticles mPEG350– and mPEG2000-coated: cell uptake and biocompatibility evaluation. Nanomed-Nanotech Nol 4:909–919
23. Maria C, Barbara DB, Maria GA, Flavia B, Giancarlo C (2016) ZnO nanoparticle tracking from uptake to genotoxic damage in human colon carcinoma cells. Toxicol In Vitro 35:169–179
24. Geng HJ, Zhao YT, Liu J et al (2016) Hollow mesoporous silica as a high drug loading carrier for regulation insoluble drug release. Int J Pharm 510:184–194
25. Wan L, Wang XF, Zhu WQ et al (2015) Folate-polyethylenimine functionalized mesoporous carbon nanoparticles for enhancing oral bioavailability of paclitaxel. Int J Pharm 484:207–217
26. Jaganathan H, Godin B (2012) Biocompatibility assessment of Si-based nano- and micro-particles. Adv Drug Deliv Re 64:1800–1819
27. Minati L, Antonini V, Serra MD et al (2013) pH activated doxorubicin release from polyelectrolyte complex layer coated mesoporous silica nanoparticles. Micropor Mesopor Mat 180:86–93
28. Vishnu SB, Ayan KB, Sujan KM et al (2016) Curcumin-loaded silica-based mesoporous materials: synthesis, characterization and cytotoxic properties against cancer cells. Mat Sci Eng C-Mater 63:393–410
29. Zhao LL, Kim TH, Kim SW, Ahn JC, Yoon SY (2016) Enhanced cellular uptake and phototoxicity of Verteporfin-conjugated gold nanoparticles as theranostic nanocarriers for targeted photodynamic therapy and imaging of cancers. Mat Sci Eng C-Mater 67:615–622